



From Behavior of Water on Hydrophobic Graphene Surfaces to Ultra-Confinement of Water in Carbon Nanotubes

Alia Mejri, Guillaume Herlem, Fabien Picaud

► To cite this version:

Alia Mejri, Guillaume Herlem, Fabien Picaud. From Behavior of Water on Hydrophobic Graphene Surfaces to Ultra-Confinement of Water in Carbon Nanotubes. *Nanomaterials*, 2021, 11 (2), pp.306. 10.3390/nano11020306 . hal-04189066

HAL Id: hal-04189066

<https://hal.science/hal-04189066>

Submitted on 28 Aug 2023

HAL is a multi-disciplinary open access archive for the deposit and dissemination of scientific research documents, whether they are published or not. The documents may come from teaching and research institutions in France or abroad, or from public or private research centers.

L'archive ouverte pluridisciplinaire **HAL**, est destinée au dépôt et à la diffusion de documents scientifiques de niveau recherche, publiés ou non, émanant des établissements d'enseignement et de recherche français ou étrangers, des laboratoires publics ou privés.



Article

From behavior of water on hydrophobic graphene surface to ultra-confinement of water in carbon nanotube

Alia MEJRI¹, Guillaume HERLEM¹ and Fabien PICAUD ^{1,*}¹ Laboratoire de Nanomédecine, Imagerie et Thérapeutiques, EA4662, UFR Sciences et Techniques, Centre Hospitalier Universitaire et Université de Bourgogne Franche Comté, 16 route de Gray, 25030 Besançon

* Correspondence: fabien.picaud@univ-fcomte.fr

Abstract: Since few years and the achievement of the nanotechnologies, the development of experiments based on carbon nanotube has allowed to increase the ionic permeability and/or selectivity in nanodevices. However, this new technology opens the way to a lot of questionable observations, for which theoretical works are able to answer using several approximations. One of these concerns the apparition of a negative charge on the carbon surface, while this latter is apparently neutral. Using first principles functional density theory combined to molecular dynamics, we develop here several simulations on different systems in order to understand the reactivity of the carbon surface in low or ultra-high confinement. Our calculations demonstrate the high affinity of the carbon atom in every situation only for hydrogen ion, and in a less extend, for hydroxyl ion. This latter can only occur when the first hydrogen attack has been achieved. As a consequence, the functionalization of the carbon surface upon the presence of a water media is activated by its protonation, then allowing reactivity of anion.

Keywords: Quantum simulations, carbon nanotube, graphene, functionalization, confinement.

Citation: Mejri, A.; Herlem, G.;

Picaud, F. From behavior of water on hydrophobic graphene surface to ultra-confinement of water in carbon nanotube. *Nanomaterials* **2021**, *11*, x. <https://doi.org/10.3390/xxxxx>

Received: date

Accepted: date

Published: date

Publisher's Note: MDPI stays neutral with regard to jurisdictional claims in published maps and institutional affiliations.



Copyright: © 2020 by the authors.

Submitted for possible open access

publication under the terms and

conditions of the Creative Commons

Attribution (CC BY) license

(<http://creativecommons.org/licenses/by/4.0/>).

1. Introduction

Several curved and flat solid structures such as carbon (CNT) [1-6], boron nitrides (BNNT) and silicon carbide [7,8] nanotubes or surfaces [9,10] (graphene [11-16]) are interesting candidates for the design of synthetic nanofluidic platforms. The easy control of their diameter during synthesis process can regulate inside liquid flow and transport of charges opening up a wide field of applications in nanomedicine [17-19], biotechnology, desalination [20-23] membrane nanofiltration [24,25] nanofluidic devices for energy recovery and conversion [26-32] and water filtration [33]. CNTs are able to reproduce the biological properties of their counterparts, but with a less complex composition. For instance, they can notably present a chemical selectivity such as some natural nanochannels or transport different species. Many other different properties of bulk fluids could be also observed in such systems due to the surface effect.

Simulations and experiments with water confined inside carbon nanotubes can reveal unusual physical properties, especially for diffusion behavior and viscosity. These properties are highly dependent on the geometrical characteristics of the CNT (tube diameter and chirality) and can directly affect water distribution inside the cage leading to unusual water performance in confined space [34-40]. Several studies have shown for CNTs and BNNTs an ordered structure of water molecules essentially related to the metallicity and diameter of the tube. Pascal et al. reported that for armchair CNTs with increased diameters, water molecules present a bulk-like behavior when CNTs diameter is above 1.4 nm, while an ice-like framework water is characterized for CNTs diameters ranging from 1.1 and 1.2 nm [41]. In a recent theoretical study, molecular dynamic simulations

reveal that network formation in the form of a water chain-like occurs where molecules are successively arranged in CNT of diameters around 1.1 nm [39], which is in accordance with several previous studies [35,42–44]. Shayeganfar et al. reported, thanks to ab initio computations, that a water tube shape is observed when confined in CNTs and BNNTs. They also confirmed that this tendency of water arrangement depends on the diameter for both situations [45].

Otherwise, numerous experimental and theoretical studies carried out in recent years have shown that a significant surface charge in both carbon and BN walls occurs in nanofluidic transport systems [9,46]. It has been established that this surface charge can be much higher for BNNT tubes than for CNTs. A plausible explanation for the appearance of this surface charge has remained puzzling. But most of the available studies suggest that the adsorption of hydroxide ions on hydrophobic surfaces could explain this phenomenon.

Sirin et al. have shown in an experimental study that the high surface charge measured on a BNNT connecting two reservoirs could be related to the diameter of the tube as well as to the pH of the studied medium. The hypothesis of a chemical reactivity at the surface of the BNNT has therefore been underlined. Based on previous theoretical studies, it has been proposed that a site of “activated” boron can indeed cause the dissociation of water on the BN sheet [47,48]. Note also that carbon structures could also, both at the theoretical and experimental scales, show a particular ionic selectivity as a function of their diameter and chirality [49,50], which could explain the specific charges of the carbon walls.

The good understanding of the mechanism governing the transport of fluid inside carbon-based materials, at the theoretical scale, would be an essential step in the development of new generation devices for a wide field of new industrial applications.

In fact, simulating the behavior of water molecules towards nanoporous solids is of great interest to investigate promising materials for smart nanofluidic systems under electric bias [51–54]. Consequently, recourse to computational methods would make it possible to establish a realistic approach by reproducing an electrochemical system in which the electrolytes are in contact with a solid polarized surface under the effect of an external uniform electric field [2,55,56].

Otani and O. Sugino [57] have developed since 2006 a novel computational scheme which makes it possible to apply an electric bias to the system constituting of a slab as occurring with an electrode and an electrolyte solution. The slab represents a bounded polarized or charged interface between two semi-infinite media having a dielectric constant. The method is then called « Effective Screening Medium ». The boundary conditions are given to a model unit cell by solving the Poisson equation allowing the creation of an infinite slab.

The Effective Screening Medium (ESM) method allows, through the coupling of DFT and molecular dynamics, a rigorous study of electrochemical systems. In the present study, two solid structures were tested against dissociated and undissociated water: the zigzag carbon nanotube and the graphene monolayer. Various quantities were then extracted from this study, in particular the adsorption energy of water on the solid surface, the radial distribution density of the confined water as well as the relevant structural observations.

2. Materials and Methods

First principles Functional Density theory calculations were used to investigate the interaction of a dissociated and undissociated water molecule with graphene and the carbon nanotube. The geometry optimization was performed through the « Open source package for Material eXplorer code » (OpenMX) using a combination of molecular dynamics and local density approximation (LDA) for the exchange-correlation potentials with the Perdew–Burke–Ernzerhof (PBE) functional. Pseudopotentials and wave functions have also been implemented to reduce the calculations cost. An investigation of the structural and energetical properties was performed on the studied systems such as adsorption energy, ground state geometries of system components, and electronic density of states (DOS). Differences in charge density calculations were also performed by OpenMX code for the adsorption of dissociated water molecules to CNT and graphene structures. This implies a more rigorous understanding of the spin (charges) density redistribution induced by the interaction of water entities with carbon structures.

The total energy self-consistent convergence criterion for the self-consistent electronic minimization is set at 10^{-6} hartree. Pseudo-atomic orbitals (PAOs) centered on atomic sites were used as basis sets. The basis sets for C, O, Cl, B, N were taken as “s2p2d1”, while those for Na atoms were “s2p2”. The k points are generated according to the Monkhorst-Pack method, and were set to $3 \times 3 \times 1$. The mesh cut-off energy value was set to 170 Ry. Otherwise, a large 34 Å vacuum is built into the cell along the z axis to avoid overlapping periodic cells.

The adsorption energy (equation 1) is estimated based on a difference between the total energy of the complex tube CNT (and graphene) + adsorbate system and the individual tube (and graphene) and gas phase free molecule system.

$$E_{\text{ads}} \text{ H}^+/\text{OH}^- = E_{\text{tot}} (\text{H}^+/\text{OH}^- \text{ ads_surface}) - E(\text{H}^+/\text{OH}^- \text{ des_surface}) \quad (1)$$

For all the simulations, molecular dynamics calculations were carried out in the NVT_VS ensemble at 300 K. The velocities of the atoms were scaled every 20 MD steps and time step is of 1 fs. All simulations were run for 2000 fs.

Monolayer graphene is made of 32 atoms and adopts an armchair chirality (1,1) with honeycomb structure, and semi-metallic properties. The monolayers of each system are separated by a 34 Å vacuum to avoid any interaction between the periodic images.

Carbon nanotubes have been also studied with a confined water molecule and the same vacuum exclusive region as previously. For all the structures, two situations are investigated: a first case with an undissociated water molecule and a second one with a dissociated water molecule. In each situation, the cases without field and with field application are also explored.

3. Results

3.1. Water molecule interaction with graphene walls

Graphene has become a key component in the development of graphitic nanoslits for the transport of water and ion [58–60]. But there is still an important lack in the theoretical studies which analyze the behavior of water towards this material since many experimental observations are still interpreted as coming from the apparition of a surface charge. The origin of this latter needs a more profound theoretical insight to understand its appearance. Hence, it seemed relevant to investigate more closely the behavior of a dissociated water molecule near a single graphene sheet. An uniform electric field is applied to the system to model the influence of the potential drop used in current-voltage measurements. Figure 1 shows the system studied, and summarizes the ESM method model used in these calculations.

The same calculations were also performed for an undissociated water molecule, the applied field did not cause the spontaneous dissociation of the water molecule even for high intensities.

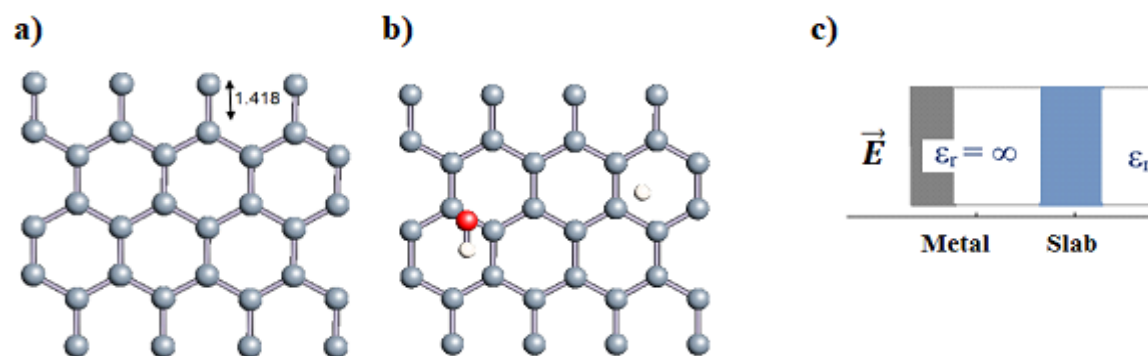


Figure 1. a, b) Graphene and dissociated water + graphene system. c) ESM method model.

As shown in Table 1, which summarizes all the adsorption energies of H^+ and OH^- on the graphene surface due to the most important events occurring during the simulation, the adsorption states of H^+ and HO^- are all negative indicating favorable adsorption in each case. The first adsorption energy of each entity is called E_{ads} . H^+ and E_{ads} HO^- .

In the three 2000 fs simulations, the adsorption of the H^+ is noted at fast times. For fields equal to 0 eV and -5 eV, HO^- adsorption was not observed. A very high field intensity, only, lets the adsorption of HO^- occurs.

Table 1. Adsorption states and energies of dissociated water molecule on graphene monolayer.

U(eV)	0	-5	-50
Figure			
Observation	H^+ adsorption at 79 fs H_2O formation at 365 fs.	H^+ adsorption at 63 fs H_2O formation at 365 fs	H^+ adsorption at 40 fs HO^- adsorption at 906 fs
Eads. H^+ (eV)	-0.9	-1.3	-1.5
Eads. HO^- (eV)	-	-	-0.6

The hydrogen adsorption energies are in agreement with the theoretical calculations observed in the literature which ranged from -0.81 [61] for the PBE method to -0.67 in LSDA [62].

The adsorption energy of HO^- is not favored in the first two situations, when the electric field value is of low intensity. It can only occur with a strong field but presents a value which remains in agreement with the literature for this type of systems. Note that the adsorption of HO^- is only possible after a first adsorption of H^+ thus creating a defect in the electronic structure of the planar surface. This has been already observed in recent

data since the HO- adsorption on graphene was never chemical and lead to small interaction energies with carbon atom.

To better understand the ability of the hydrogen or hydroxyl ions to interact with the graphene sheet, we represent in Figure 2, the charge density distribution differences for dissociated water molecule near graphene sheet.

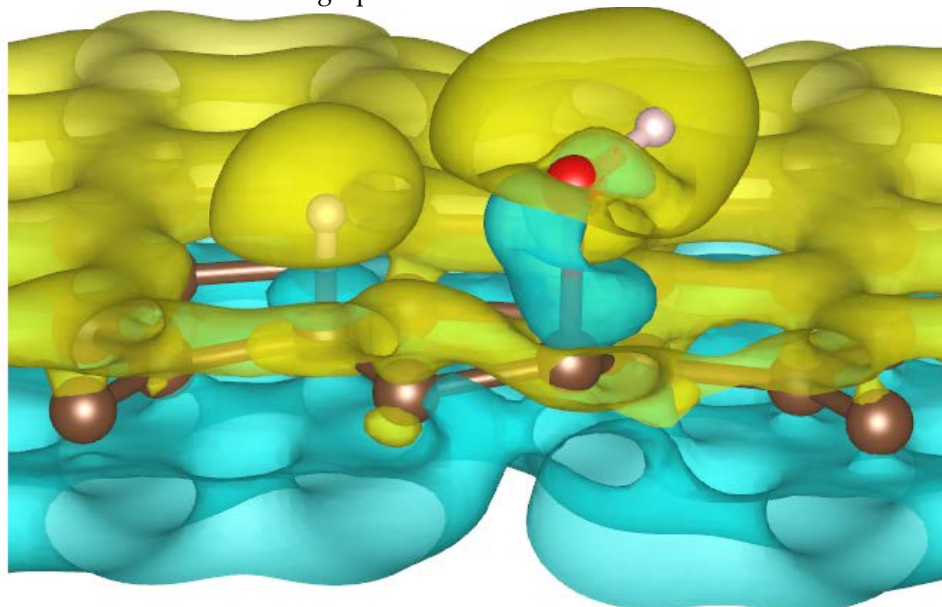


Figure 2. Charge-density distribution in case of dissociated water molecule adsorption on graphene at -50 eV electric field. Yellow and blue lobes represent respectively the positively and negatively charged areas.

As shown in Figure 2, the surface polarization generated by the effect of the electric field creates negative and positive charges on the carbon atoms of the graphene. This polarization allows H⁺ ion to be adsorbed on the carbon atoms which presents a negative surface layer. Indeed, H⁺ is forced to translate in the field direction, as the partial charges on the graphene surface do. This induces favorable adsorption of H⁺ at the first step of the simulation. Once H⁺ is linked to a carbon atom, it modifies locally the density of charge repartition. Without such changes, HO⁻ could never be adsorbed on the graphene surface. The presence of the cation allows thus to HO⁻ to be attracted by the graphene surface spontaneously.

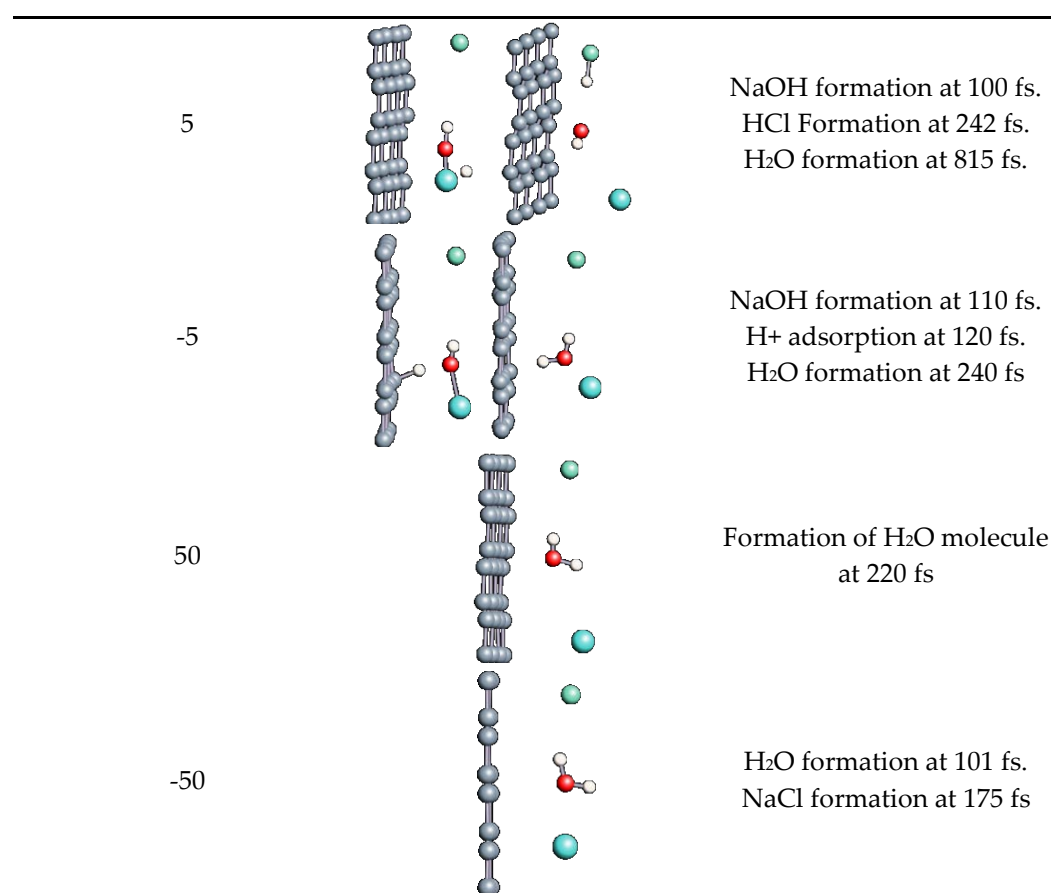
3.1.1. Salt effect

The role of salt in the water dynamic is necessary to complete the simulated system and to approximate the experimental conditions. The dissociated sodium chloride (Na⁺, Cl⁻) has thus been added to the previous system.

The behavior of water and salt with respect to graphene at different field strengths is given in Table 2.

Table 2. Behavior of dissociated water molecule near graphene layer in the presence of salt under electric bias

U(eV)	Important events in simulation	Observations
0		H ⁺ adsorption at 135 fs. H ₂ O formation at 292 fs.



In all the simulations, the reformation of water molecules from H⁺ and HO⁻ in solution is observed at relatively short times for all field intensities. However, for weak field intensities, short-lived interactions of H⁺ with the carbon surface are possible but are not really relevant. There is no a real OH⁻ and H⁺ adsorption phenomenon on the graphene surface in the presence of salt in these simulations. Note that during the simulations, the reformation of NaCl is observed close to the graphene surface in our electrochemical ESM cell. There is thus no possibility for salt ions to be kept by the graphene surface.

3.2. Undissociated water molecule inside the carbon nanotube

The role of the confinement at the nanometric scale on the possibility to charge a carbon wall was then studied. Indeed, it has been established in previous experimental and theoretical studies [63–65] that the water dissociation can occur under the effect of an electric field. Furthermore, studies of the water behavior in an ultra-confined environment have not excluded the possibility of its dissociation [66,67]. This dissociation can be very favored in a confined space, in fact, Muñoz-Santiburcio et al. have shown that confinement greatly improves the self-dissociation process of water. This result is consistent with another study conducted by Sirkin et al. who used QM/MM molecular dynamics to compute the energy without water dissociation in a single-walled carbon nanotube 8.1 Å diameter. They hypothesized that it seems plausible, under the effect of nanometric confinement, to see an increase in the self-dissociation constant due to the increase in the permittivity of the confined fluid [67]. We first modeled a (16,0) single-walled carbon nanotube with diameter equal to 1.35 nm where a water molecule is introduced in the confined inner space of the carbon cage. Several situations have been achieved by increasing the field intensity (Fig. 3).

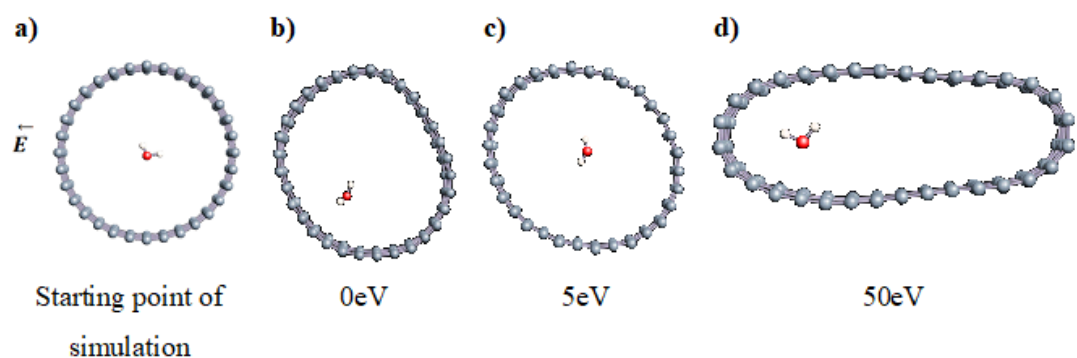


Figure 3. electrical polarization effect on water@tube system.

Despite the importance of the applied field intensities which strongly impact the geometry of the carbon nanotube, we did never observe any dissociation of confined water molecule. There is a deformation of the nanotube until it becomes crushed and takes an elongated shape in the transverse direction (Fig. 3d). Whatever the deformation, the molecule diffuses inside the inner volume of the CNT, exploring different atomic positions but keeping its distance from carbon wall due to hydrophobic interaction.[68] Note that no form of physical or chemical adsorption of the water molecule is noted on the carbon surface.

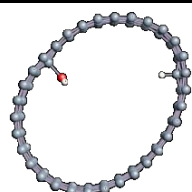



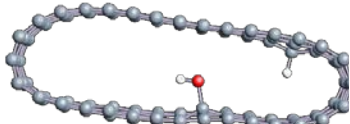
3.2.1. Dissociated water molecule inside CNT

Since no dissociation of the molecule was achieved under the action of an electric field or not in our previous modelization, the next step of our calculations deals with the simulation of a dissociated water molecule inside the carbon cage. In this case, we study directly the possibility of hydronium and hydroxyl ions adsorption resulting from this dissociation and quantify it in terms of adsorption energy. Several simulations were undertaken for a dissociated water molecule confined inside the carbon nanotube (16,0). The main results are shown in Table 3 and 4.

We first noted that the H^+ adsorption is possible spontaneously without any external contribution of an electric field as seen for the first simulation at 0 eV field intensity. In addition, our calculations show that the adsorption of H^+ always precedes that of HO^- regardless the intensity of the applied field. Note here that the hydrogen adsorption is favored rapidly and did not depended on the deformation of the carbon cage under the electric field intensity. The rapid process leading to the hydrogenation of a carbon has been observed before the strong modification of the carbon geometry. On the contrary, the formation of water molecule (observed for $E=10\text{eV}$) or the adsorption of hydroxyl is only possible when H^+ is chemisorbed and carbon surface is deformed under increasing electric field intensity, as observed previously.

Table 3. water molecule dissociated inside (16,0) CNT under electric bias.

U(eV)	Important events in simulation	Observations
0		H^+ adsorption at 140 fs.

1		H ⁺ adsorption at 112 fs. HO ⁻ adsorption at 212 fs.
5		H ⁺ adsorption at 113 fs.
10		H ⁺ adsorption at 110 fs. H ₂ O formation at 456 fs
15		H ⁺ adsorption at 95 fs HO ⁻ adsorption at 470 fs
25		H ⁺ adsorption at 104 fs HO ⁻ adsorption at 589 fs

The last two simulations gathered in Table 3 (performed at 15 eV and 25 eV) recall the case of graphene for a dissociated water molecule. In fact, HO⁻ adsorption takes place at later times in the simulation but especially at high field intensities and for an important carbon deformation. We reported in Table 4 the different adsorption energies obtained when hydrogen and/or hydroxyl ions are adsorbed on the carbon wall.

Table 4. (H⁺, HO⁻) Adsorption energies inside (16,0) CNT

U(eV)	H ⁺ Ads. energy (eV)	HO ⁻ ads. energy (eV)
0	-4.1	-
1	-4.2	-0.3
5	-4.0	-
10	-4.6	-
15	-4.6	-0.06
20	-4.3	-
25	-4.2	-0.3

The energies calculated for H⁺ adsorption in the inner surface of the carbon cage are of the order of -4 eV. These clearly show that the adsorptions observed are chemisorptions, explaining the difficult for hydroxyl ion to interact with hydrogen once chemisorbed. These values remain in agreement with other found in the literature which ranged around -3eV [69]. Note also that for each modification of the carbon surface by the hydrogen chemisorption, we observed a modification of the carbon hybridation which could be apparent to a sp³ mode. The hydroxyl ion interacted with the carbon surface with a higher energy, which remains comparable with those obtained in the literature. [70]

3.2.2 Differences in charge density distribution for the dissociated water molecule inside CNT

In figure 4, we plot the modification of the atomic charge density with time upon the application of high electric field intensity (25 eV). The positive and negative differences in total charge densities are colored in yellow and blue, respectively. As seen in Fig. 4, the polarization of the surface is responsible for the delocalization of electrons and therefore for the creation of an electron deficit on certain areas of the internal surface of the tube and an accumulation of electrons in other areas. As a consequence, the hydrogen ion will be more sensitive to the surface zone where the electrons are present while the hydroxyl remains close to surface part charged in an opposite way. However, even in this large field intensity, the time necessary to obtain the hydroxyl binding to the carbon surface is quite large (627 fs) while hydrogen ion is attached faster to the surface (85 fs compared to 110 fs at least).

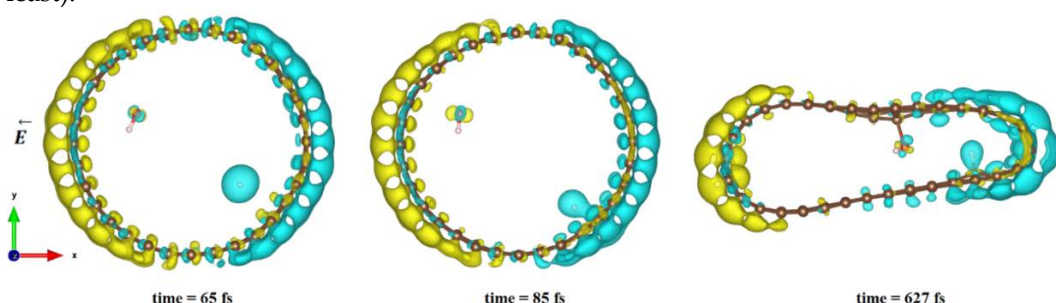


Figure 4. Difference in charge density distribution of the dissociated water molecule inside the CNT under 25 eV electric field. The yellow and blue lobes represent the positively and negatively charged areas, respectively.

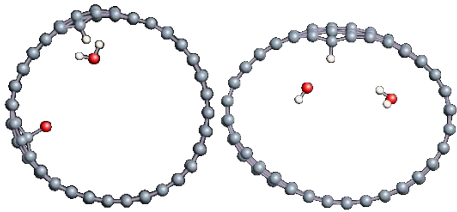
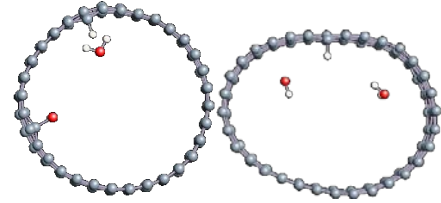
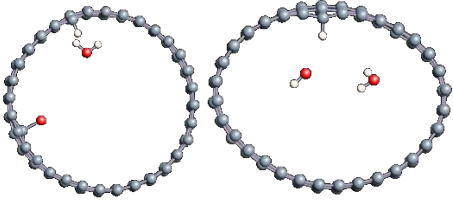
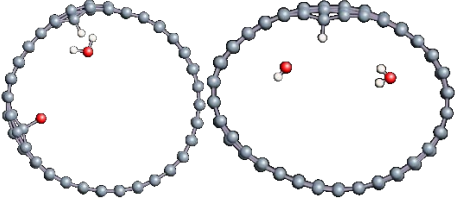
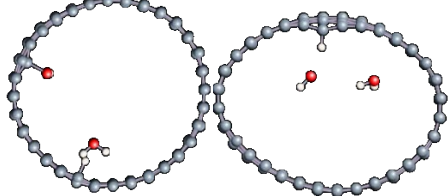
3.2.3. Effect of adding water molecules on the adsorption steps

To go further in our study, we complicated the previous system by adding an additional water molecule and let the system evolve to see its effect on the adsorption steps. Several simulations were performed by varying the intensity of the applied field. A domain of intensities ranging from 0 to 30 eV was scanned. Table 5 illustrates all the simulations carried out for this system containing one dissociated and one undissociated water molecule inside the carbon nanotube (16,0).

As shown in Table 5, the same behavior is almost detected in all the simulations, even at high field strengths. The phenomena of H^+ and HO^- adsorption occurs at practically simultaneous instants with a very slight advance of HO^- adsorption of a few fs over the H^+ adsorption, compared to the previous system. This first HO^- adsorption, before any other, is the main difference obtained in this system which has never been observed previously. However, it is not very durable because the entity is desorbed in all cases after 40 fs of existence, depicting a very low adsorption energy with carbon atom. On the other hand, H^+ remains adsorbed until the end of the simulation in all situations, as observed previously. We may thus question on the role of HO^- on the H^+ adsorption in this case. It can either be the main factor which improved the association of hydrogen with carbon by the modification of the electronic structure of the cage or, simply, be the random consequence of the hydroxyl position compared to the hydrogen position. Note that no dissociation of the water molecule has been observed during the simulation.

Table 5. Dissociated and undissociated water molecules inside (16,0) CNT under electric bias

308

Field intensity (eV)	Important events	Observation
1		134 fs HO ⁻ adsorb 150 H ⁺ 179 HO ⁻ desorption
10		135 HO ⁻ 137 H ⁺ 173 HO ⁻ desorption
15		133 HO ⁻ 137 H ⁺ 167 HO ⁻ desorption
20		133 HO ⁻ 138 H ⁺ 173 HO ⁻ desorption
30		133 HO ⁻ 136 H ⁺ 177 HO ⁻ desorption

309

310

311

312

313

314

315

316

Adsorption energies were calculated. Results are reported in Table 6. Due to very fast hydroxyl adsorption events, we were not able to estimate precisely the adsorption energy for HO⁻ ion. However, as seen in Table 6, the hydrogen adsorption energy remains equal to -4.4 eV as obtained previously (Table 4) for the system where no water molecule was present in the system. The role of the water molecule added to the hydrogen plus hydroxyl ion seems to play a minor role in the reactivity of the carbon surface.

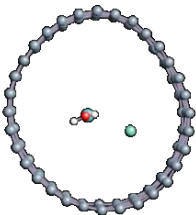
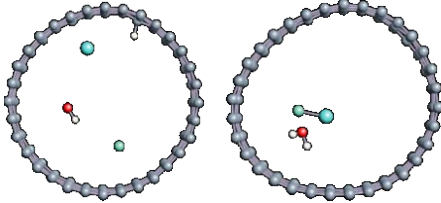
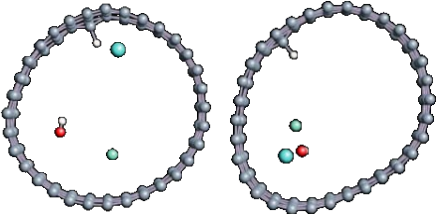
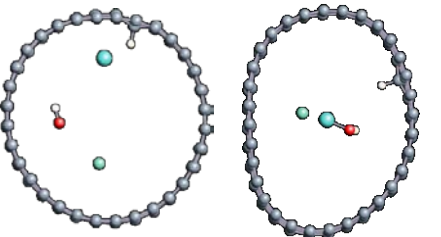
Table 6. H⁺ Adsorption energies inside (16,0) CNT

U(eV)	H ⁺ Ads. energy (eV)
1	-4.413
10	-4.408
15	-4.426
20	-4.409
30	-4.508

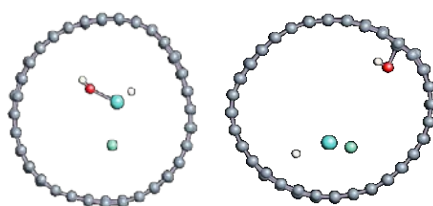
3.2.4. Salt effect on adsorption phenomena

In order to evaluate the effect of ions on the adsorption of dissociated water inside carbon nanotube, we added to the dissociated H₂O @ CNT system, a salt composed of a unique Na⁺ ion and its counterion Cl⁻. The different adsorption events as a function of the increasing field intensity are summarized in Table 7. For intensities between 5 and 20 eV, H⁺ adsorption first occurs at around 80 fs followed by the rapid reformation of the water molecule. At a field of 25 eV, HO⁻ adsorption occurs first, at about 385 fs and the entity remains adsorbed for 200 fs. Note that CNT is much less deformed under the action of an intense electric field when it contains more molecules and that no dissociation of water molecule is observed once formed.

Table 7. Dissociated water molecules inside (16,0) CNT under electric bias in presence of a salt.

Field Intensity (eV)	Important events in simulation	Observations
0		H ₂ O is formed at 250 fs
5		H ⁺ adsorbed at 75 fs H ₂ O is formed at 551 fs
10		H ⁺ is adsorbed at 90 fs and HO ⁻ remains free until the end of the simulation
20		H ⁺ is adsorbed at 83 fs and HO ⁻ remains free until the end of the simulation. NaOH formation.

25



NaOH formation at 268 fs.

HO⁻ adsorption at 385 fs.HO⁻ desorption at 556 fs.

As for other systems, we estimate the H⁺ and HO⁻ adsorption energies in Table 8. We observe that the adsorption of H⁺ is less favorable in this case (-4 eV at best) while the adsorption of HO⁻ in the very high electric field intensity is of the same order than the H⁺ one. The rapid desorption of HO⁻ cannot explain this result but the presence of Na⁺ allows it. Indeed, we observe an important role played by the salt which are alternatively attracted by either hydrogen or hydroxyl ions in order to form another strong acid or base component.

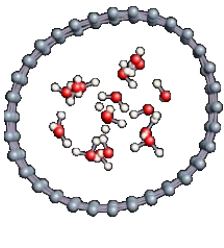
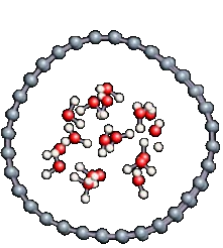
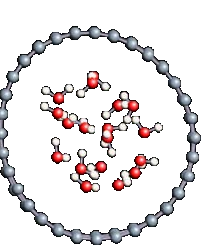
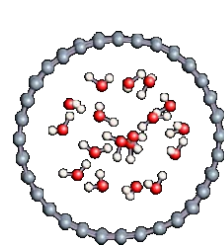
Table 8. H⁺ Adsorption energies inside (16,0) CNT in presence of salt

U(eV)	H ⁺ Ads. energy (eV)	H ⁺ Ads. duration (fs)	HO ⁻ ads. energy (eV)	HO ⁻ ads. duration (fs)
0	-	-	-	-
5	-3.288	476	-	-
10	-3.449	1910	-	-
20	-4.087	1917	-	-
25	-	-	-3.211	171

3.2.5. Several water molecules inside (16,0) carbon nanotube

In order to get closer to biological conditions, a system with dissociated water molecule submersed in several water molecules is simulated by varying the intensity of the applied electric field. The density of water has been calculated to 1 in order to reproduce a bulk like water media. After 2000 fs simulations we observe in all cases a rapid formation of water molecule (in 17 fs).

Table 9. distribution of water inside the (16,0) carbon nanotube

Field intensity (Ev)	0	10	25	50
Water distribution				
First maximum position (Å)	2.66	2.73	2.75	2.75

In order to check the conformation of the confined water and to see if possibly a phase change has taken place, we calculated the radial distribution density of the water in the various studied situations. The calculated values are entered as the water at the end of the

simulation keeps the structure of the liquid phase and summarized in Table 10. For each case, the first peak is localized at nearly 2.7 Å. This value corroborates the organization of the water molecule as a liquid since the experimental value for liquid water which is 2.88 Å.

Table 10. First peak position in the radial distribution function of confined water.

U(eV)	First maximum position (Å)
0	2.658
10	2.73
25	2.754
50	2.75

Experimental Value for liquid water g_{OO1}= 2.88

Note that during the simulation, while no adsorption was observed on the carbon surface, the formation of successive hydronium ion inside the water bulk and proton jump have been effective via the so-called Grotthuss mechanism.

3.3. Change in hybridization of the adsorption site

We found by comparing the two carbon structures that the adsorption of HO⁻ on carbon nanotubes is much more favorable than on graphene monolayer and takes place at lower field intensities. This is probably due to the higher surface charge of the carbon nanotube and its coiled structure.

We noted here for the carbon structures, that a change of conformation is observed for the carbon atom at the adsorption site (see figure 5). Indeed, as established by previous studies, the adsorption of an entity on a graphene surface or on the internal or external surface of a single-walled carbon nanotube modified the adsorption site initially hybridized sp² (planar structure). Due to the adsorption it deviates from its original state towards sp³ type hybridization. It is then the center of a regular tetrahedron defined by three adjacent carbon atoms and the adsorbed entity. This strong local deformation causes a change in the bond angles of the original sp² hybridization (CCC) = 120° to (CCC) = 112° respectively for CNT and graphene.

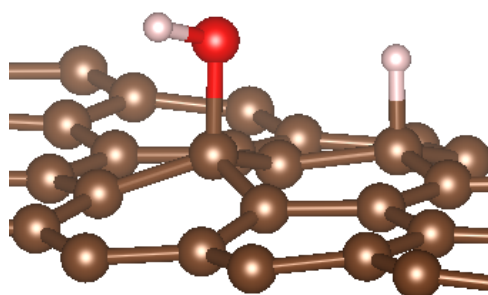


Figure 5. sp³ hybridization of the adsorption site for graphene material.

Note also that the observed bond lengths are C-H_{graphene} = 1.1 Å; C-H_{CNT} = 1.12 Å; C-O_{graphene} = 1.52; C-O_{CNT} = 1.496 Å, which are very characteristic of single bonds for each of the studied structures. The puckering of the carbon atom beneath the adsorbed

hydrogen atom, leads to an increase in its sp^3 character [9,13,15,69,71-76]. A stretching in the C-C bonds associated with this carbon atom is also noted. They are approximately 0.3 Å elongated from the original C-C bond length in pure structures. Casolo et al. quantified the electronic rearrangement of the carbon atom by a high energy barrier of 0.2 eV [71,77].

5. Conclusions

In this work, we studied through DFT-MD calculations the analysis of flat (graphene) or curved (CNT) carbon surface reactivities to proton and hydroxyl ions or hydroxyl ions, mixed or not with other entities, upon the presence of an electric field or not at the molecular scale. From all of our studies, we demonstrated here a very strong affinity of the carbon wall, whatever its curvature, for proton, with a notable modification of the hybridization of carbon atom. The adsorption energy obtained in each case is about -4eV, in agreement with literature. On the contrary, we can note that no specific adsorption preferences have been characterized for HO^- ion. Some punctual observations of hydroxyl interaction with the carbon surface have been obtained, but mainly after a first functionalization of the carbon by the hydrogen in the presence and absence of an electric field. However, the higher the electric field intensity, the faster the proton chemisorption rate. For graphene, the presence of a dissociated salt (NaCl) with water lead to desorption of ions, while HO^- can adsorb first as observed in CNT charged with NaCl. This asymmetry of ion adsorptions occurs on flat and curved carbonaceous surfaces but can be drastically affected by an external electric field, while being pH dependent in water.

Author Contributions: “Conceptualization and methodology, A.M., G.H. and F.P.; simulation, A.M.; writing—original draft preparation, A.M.; writing—review G.H. and F. P. and editing, F.P. All authors have read and agreed to the published version of the manuscript.”

Acknowledgments: This work was founded by Agence Nationale de la Recherche (ANR-18-CE09-0011-01 “IONESCO”). Single tracks have been produced in GANIL (Caen, France) in the framework of an EMIR project. Calculations were performed at the supercomputer regional facility Mesocentre of the University of Franche-Comté with the assistance of K. Mazouzi. This work was also granted access to the HPC resources of IDRIS, Jean Zay supercomputer, under the allocation 2019 - DARI A0070711074 made by GENCI. Finally, part of this work was performed using computing resources of CRIANN (Normandy, France).

Conflicts of Interest: “The authors declare no conflict of interest.”

References

1. Vaitheeswaran, S.; Rasaiah, J.C.; Hummer, G. Electric field and temperature effects on water in the narrow nonpolar pores of carbon nanotubes. *The Journal of Chemical Physics* **2004**, *121*, 7955-7965, doi:10.1063/1.1796271.
2. Mikami, F.; Matsuda, K.; Kataura, H.; Maniwa, Y. Dielectric Properties of Water inside Single-Walled Carbon Nanotubes. *ACS Nano* **2009**, *3*, 1279-1287, doi:10.1021/nn900221t.
3. Kyakuno, H.; Fukasawa, M.; Ichimura, R.; Matsuda, K.; Nakai, Y.; Miyata, Y.; Saito, T.; Maniwa, Y. Diameter-dependent hydrophobicity in carbon nanotubes. *The Journal of Chemical Physics* **2016**, *145*, 064514, doi:10.1063/1.4960609.
4. Hassan, J.; Diamantopoulos, G.; Homouz, D.; Papavassiliou, G. Water inside carbon nanotubes: structure and dynamics. *Nanotechnology Reviews* **2016**, *5*, 341, doi:https://doi.org/10.1515/ntrev-2015-0048.

5. Yao, Y.-C.; Taqieddin, A.; Alibakhshi, M.A.; Wanunu, M.; Aluru, N.R.; Noy, A. Strong Electroosmotic Coupling Dominates Ion Conductance of 1.5 nm Diameter Carbon Nanotube Porins. *ACS Nano* **2019**, *13*, 12851–12859, doi:10.1021/acsnano.9b05118.
6. Thiruraman, J.P.; Masih Das, P.; Drndić, M. Ions and Water Dancing through Atom-Scale Holes: A Perspective toward “Size Zero”. *ACS Nano* **2020**, *14*, 3736–3746, doi:10.1021/acsnano.0c01625.
7. Khademi, M.; Sahimi, M. Molecular dynamics simulation of pressure-driven water flow in silicon-carbide nanotubes. *The Journal of Chemical Physics* **2011**, *135*, 204509, doi:10.1063/1.3663620.
8. Barghi, S.H.; Tsotsis, T.T.; Sahimi, M. Hydrogen sorption hysteresis and superior storage capacity of silicon-carbide nanotubes over their carbon counterparts. *International Journal of Hydrogen Energy* **2014**, *39*, 21107–21115, doi:https://doi.org/10.1016/j.ijhydene.2014.10.087.
9. Grosjean, B.; Pean, C.; Siria, A.; Bocquet, L.; Vuilleumier, R.; Bocquet, M.-L. Chemisorption of Hydroxide on 2D Materials from DFT Calculations: Graphene versus Hexagonal Boron Nitride. *The Journal of Physical Chemistry Letters* **2016**, *7*, 4695–4700, doi:10.1021/acs.jpclett.6b02248.
10. Comtet, J.; Grosjean, B.; Glushkov, E.; Avsar, A.; Watanabe, K.; Taniguchi, T.; Vuilleumier, R.; Bocquet, M.-L.; Radenovic, A. Direct observation of water-mediated single-proton transport between hBN surface defects. *Nature Nanotechnology* **2020**, *15*, 598–604, doi:10.1038/s41565-020-0695-4.
11. Striolo, A.; Chialvo, A.A.; Cummings, P.T.; Gubbins, K.E. Water Adsorption in Carbon-Slit Nanopores. *Langmuir* **2003**, *19*, 8583–8591, doi:10.1021/la0347354.
12. Cole, D.J.; Ang, P.K.; Loh, K.P. Ion Adsorption at the Graphene/Electrolyte Interface. *The Journal of Physical Chemistry Letters* **2011**, *2*, 1799–1803, doi:10.1021/jz200765z.
13. Wang, Y.; Qian, H.-J.; Morokuma, K.; Irle, S. Coupled Cluster and Density Functional Theory Calculations of Atomic Hydrogen Chemisorption on Pyrene and Coronene as Model Systems for Graphene Hydrogenation. *The Journal of Physical Chemistry A* **2012**, *116*, 7154–7160, doi:10.1021/jp3023666.
14. Park, H.G.; Jung, Y. Carbon nanofluidics of rapid water transport for energy applications. *Chemical Society Reviews* **2014**, *43*, 565–576, doi:10.1039/C3CS60253B.
15. Chawla, J.; Kumar, R.; Kaur, I. Carbon nanotubes and graphenes as adsorbents for adsorption of lead ions from water: a review. *Journal of Water Supply: Research and Technology-Aqua* **2015**, *64*, 641–659, doi:10.2166/aqua.2015.102.
16. Xie, Q.; Alibakhshi, M.A.; Jiao, S.; Xu, Z.; Hempel, M.; Kong, J.; Park, H.G.; Duan, C. Fast water transport in graphene nanofluidic channels. *Nature Nanotechnology* **2018**, *13*, 238–245, doi:10.1038/s41565-017-0031-9.
17. Gao, W.; Kong, L.; Hodgson, P. Atomic interaction of functionalized carbon nanotube-based nanofluids with a heating surface and its effect on heat transfer. *International Journal of Heat and Mass Transfer* **2012**, *55*, 5007–5015, doi:https://doi.org/10.1016/j.ijheatmasstransfer.2012.04.044.
18. Goenka, S.; Sant, V.; Sant, S. Graphene-based nanomaterials for drug delivery and tissue engineering. *Journal of controlled release : official journal of the Controlled Release Society* **2014**, *173*, 75–88, doi:10.1016/j.jconrel.2013.10.017.
19. Mejri, A.; Delphine, V.; Tangour, B.; Gharbi, T.; Picaud, F. Encapsulation Into Carbon Nanotubes and Release of Anticancer Cisplatin Drug Molecule. *The journal of physical chemistry. B* **2014**, *119*, doi:10.1021/jp5102384.
20. Corry, B. Designing Carbon Nanotube Membranes for Efficient Water Desalination. *The Journal of Physical Chemistry B* **2008**, *112*, 1427–1434, doi:10.1021/jp709845u.

21. Dai, H.; Xu, Z.; Yang, X. Water Permeation and Ion Rejection in Layer-by-Layer Stacked Graphene Oxide Nanochannels: A Molecular Dynamics Simulation. *The Journal of Physical Chemistry C* **2016**, *120*, 22585–22596, doi:10.1021/acs.jpcc.6b05337.
22. Suss, M.E.; Porada, S.; Sun, X.; Biesheuvel, P.M.; Yoon, J.; Presser, V. Water desalination via capacitive deionization: what is it and what can we expect from it? *Energy & Environmental Science* **2015**, *8*, 2296–2319, doi:10.1039/C5EE00519A.
23. Wang, X.; Shi, G.; Liang, S.; Liu, J.; Li, D.; Fang, G.; Liu, R.; Yan, L.; Fang, H. Unexpectedly High Salt Accumulation inside Carbon Nanotubes Soaked in Dilute Salt Solutions. *Physical Review Letters* **2018**, *121*, 226102, doi:10.1103/PhysRevLett.121.226102.
24. Williams, C.D.; Carbone, P. Selective Removal of Technetium from Water Using Graphene Oxide Membranes. *Environmental Science & Technology* **2016**, *50*, 3875–3881, doi:10.1021/acs.est.5b06032.
25. Musielak, M.; Gabor, A.; Zawisza, B.; Talik, E.; Sitko, R. Graphene Oxide/Carbon Nanotube Membranes for Highly Efficient Removal of Metal Ions from Water. *ACS Applied Materials & Interfaces* **2019**, *11*, 28582–28590, doi:10.1021/acsami.9b11214.
26. Pumera, M. Graphene-based nanomaterials for energy storage. *Energy Environ. Sci.* **2011**, *4*, 668–674, doi:10.1039/C0EE00295J.
27. Zhai, Y.; Dou, Y.; Zhao, D.; Fulvio, P.F.; Mayes, R.T.; Dai, S. Carbon Materials for Chemical Capacitive Energy Storage. *Advanced Materials* **2011**, *23*, 4828–4850, doi:10.1002/adma.201100984.
28. Simon, P.; Gogotsi, Y. Capacitive Energy Storage in Nanostructured Carbon–Electrolyte Systems. *Accounts of Chemical Research* **2013**, *46*, 1094–1103, doi:10.1021/ar200306b.
29. Ye, J.; Simon, P.; Zhu, Y. Designing ionic channels in novel carbons for electrochemical energy storage. *National Science Review* **2019**, *7*, 191–201, doi:10.1093/nsr/nwz140.
30. Xiao, K.; Jiang, L.; Antonietti, M. Ion Transport in Nanofluidic Devices for Energy Harvesting. *Joule* **2019**, *3*, 2364–2380, doi:10.1016/j.joule.2019.09.005.
31. Feng, Y.; Zhu, W.; Guo, W.; Jiang, L. Bioinspired Energy Conversion in Nanofluidics: A Paradigm of Material Evolution. *Advanced Materials* **2017**, *29*, 1702773, doi:10.1002/adma.201702773.
32. Daiguji, H.; Yang, P.; Szeri, A.J.; Majumdar, A. Electrochemomechanical Energy Conversion in Nanofluidic Channels. *Nano Letters* **2004**, *4*, 2315–2321, doi:10.1021/nl0489945.
33. Hawks, S.A.; Cerón, M.R.; Oyarzun, D.I.; Pham, T.A.; Zhan, C.; Loeb, C.K.; Mew, D.; Deinhart, A.; Wood, B.C.; Santiago, J.G., et al. Using Ultramicroporous Carbon for the Selective Removal of Nitrate with Capacitive Deionization. *Environmental Science & Technology* **2019**, *53*, 10863–10870, doi:10.1021/acs.est.9b01374.
34. Köhler, M.H.; da Silva, L.B. Size effects and the role of density on the viscosity of water confined in carbon nanotubes. *Chemical Physics Letters* **2016**, *645*, 38–41, doi:https://doi.org/10.1016/j.cplett.2015.12.020.
35. Agrawal, K.V.; Shimizu, S.; Draushuk, L.W.; Kilcoyne, D.; Strano, M.S. Observation of extreme phase transition temperatures of water confined inside isolated carbon nanotubes. *Nature Nanotechnology* **2017**, *12*, 267–273, doi:10.1038/nnano.2016.254.
36. Fumagalli, L.; Esfandiar, A.; Fabregas, R.; Hu, S.; Ares, P.; Janardanan, A.; Yang, Q.; Radha, B.; Taniguchi, T.; Watanabe, K., et al. Anomalous low dielectric constant of confined water. *Science* **2018**, *360*, 1339–1342, doi:10.1126/science.aat4191.
37. Zaragoza, A.; Gonzalez, M.A.; Joly, L.; López-Montero, I.; Canales, M.A.; Benavides, A.L.; Valeriani, C. Molecular dynamics study of nanoconfined TIP4P/2005 water: how confinement and temperature affect

- diffusion and viscosity. *Physical Chemistry Chemical Physics* **2019**, *21*, 13653-13667, doi:10.1039/C9CP02485A.
38. de Freitas, D.N.; Mendonça, B.H.S.; Köhler, M.H.; Barbosa, M.C.; Matos, M.J.S.; Batista, R.J.C.; de Oliveira, A.B. Water diffusion in carbon nanotubes under directional electric fields: Coupling between mobility and hydrogen bonding. *Chemical Physics* **2020**, *537*, 110849, doi:https://doi.org/10.1016/j.chemphys.2020.110849.
39. Velioğlu, S.; Karahan, H.E.; Goh, K.; Bae, T.-H.; Chen, Y.; Chew, J.W. Metallicity-Dependent Ultrafast Water Transport in Carbon Nanotubes. *Small* **2020**, *16*, 1907575, doi:10.1002/smll.201907575.
40. Barati Farimani, A.; Aluru, N.R. Spatial Diffusion of Water in Carbon Nanotubes: From Fickian to Ballistic Motion. *The Journal of Physical Chemistry B* **2011**, *115*, 12145-12149, doi:10.1021/jp205877b.
41. Pascal, T.A.; Goddard, W.A.; Jung, Y. Entropy and the driving force for the filling of carbon nanotubes with water. *Proceedings of the National Academy of Sciences* **2011**, *108*, 11073, doi:10.1073/pnas.1108073108, doi:10.1073/pnas.1108073108.
42. Fu, Z.; Luo, Y.; Ma, J.; Wei, G. Phase transition of nanotube-confined water driven by electric field. *The Journal of Chemical Physics* **2011**, *134*, 154507, doi:10.1063/1.3579482.
43. Chakraborty, S.; Kumar, H.; Dasgupta, C.; Maiti, P.K. Confined Water: Structure, Dynamics, and Thermodynamics. *Accounts of Chemical Research* **2017**, *50*, 2139-2146, doi:10.1021/acs.accounts.6b00617.
44. Dalla Bernardina, S.; Paineau, E.; Brubach, J.-B.; Judeinstein, P.; Rouzière, S.; Launois, P.; Roy, P. Water in Carbon Nanotubes: The Peculiar Hydrogen Bond Network Revealed by Infrared Spectroscopy. *Journal of the American Chemical Society* **2016**, *138*, 10437-10443, doi:10.1021/jacs.6b02635.
45. Shayeganfar, F.; Beheshtian, J.; Shahsavari, R. First-Principles Study of Water Nanotubes Captured Inside Carbon/Boron Nitride Nanotubes. *Langmuir* **2018**, *34*, 11176-11187, doi:10.1021/acs.langmuir.8b00856.
46. Werkhoven, B.L.; van Roij, R. Coupled water, charge and salt transport in heterogeneous nano-fluidic systems. *Soft Matter* **2020**, *16*, 1527-1537, doi:10.1039/C9SM02144B.
47. Siria, A.; Poncharal, P.; Bianco, A.-L.; Fulcrand, R.; Blase, X.; Purcell, S.T.; Bocquet, L. Giant osmotic energy conversion measured in a single transmembrane boron nitride nanotube. *Nature* **2013**, *494*, 455-458, doi:10.1038/nature11876.
48. Zhang, L.; Chen, X. Nanofluidics for Giant Power Harvesting. *Angewandte Chemie International Edition* **2013**, *52*, 7640-7641, doi:10.1002/anie.201302707.
49. Choi, W.; Ulissi, Z.W.; Shimizu, S.F.E.; Bellisario, D.O.; Ellison, M.D.; Strano, M.S. Diameter-dependent ion transport through the interior of isolated single-walled carbon nanotubes. *Nature Communications* **2013**, *4*, 2397, doi:10.1038/ncomms3397.
50. Secchi, E.; Niguès, A.; Jubin, L.; Siria, A.; Bocquet, L. Scaling Behavior for Ionic Transport and its Fluctuations in Individual Carbon Nanotubes. *Physical Review Letters* **2016**, *116*, 154501, doi:10.1103/PhysRevLett.116.154501.
51. Su, J.; Guo, H. Control of Unidirectional Transport of Single-File Water Molecules through Carbon Nanotubes in an Electric Field. *ACS Nano* **2011**, *5*, 351-359, doi:10.1021/nn1014616.
52. Giovambattista, N.; Debenedetti, P.G.; Rossky, P.J. Effect of Surface Polarity on Water Contact Angle and Interfacial Hydration Structure. *The Journal of Physical Chemistry B* **2007**, *111*, 9581-9587, doi:10.1021/jp071957s.

53. Wang, C.; Lu, H.; Wang, Z.; Xiu, P.; Zhou, B.; Zuo, G.; Wan, R.; Hu, J.; Fang, H. Stable Liquid Water Droplet on a Water Monolayer Formed at Room Temperature on Ionic Model Substrates. *Physical Review Letters* **2009**, *103*, 137801, doi:10.1103/PhysRevLett.103.137801.
54. Wang, Z.; Ci, L.; Chen, L.; Nayak, S.; Ajayan, P.M.; Koratkar, N. Polarity-dependent electrochemically controlled transport of water through carbon nanotube membranes. *Nano letters* **2007**, *7*, 697-702, doi:10.1021/nl062853g.
55. Agrawal, B.; Singh, V.; Pathak, A.; Srivastava, R. Ab initio study of ice nanotubes in isolation or inside single-walled carbon nanotubes. *Phys. Rev. B* **2007**, *75*, doi:10.1103/PhysRevB.75.195420.
56. Elliott, J.D.; Troisi, A.; Carbone, P. A QM/MD Coupling Method to Model the Ion-Induced Polarization of Graphene. *Journal of Chemical Theory and Computation* **2020**, *16*, 5253-5263, doi:10.1021/acs.jctc.0c00239.
57. Otani, M.; Sugino, O. First-principles calculations of charged surfaces and interfaces: A plane-wave nonrepeated slab approach. *Physical Review B* **2006**, *73*, 115407, doi:10.1103/PhysRevB.73.115407.
58. Amorim, R.G.; Fazzio, A.; Antonelli, A.; Novaes, F.D.; da Silva, A.J.R. Divacancies in Graphene and Carbon Nanotubes. *Nano Letters* **2007**, *7*, 2459-2462, doi:10.1021/nl071217v.
59. Cohen-Tanugi, D.; Grossman, J.C. Water Desalination across Nanoporous Graphene. *Nano Letters* **2012**, *12*, 3602-3608, doi:10.1021/nl3012853.
60. Surwade, S.P.; Smirnov, S.N.; Vlassiouk, I.V.; Unocic, R.R.; Veith, G.M.; Dai, S.; Mahurin, S.M. Water desalination using nanoporous single-layer graphene. *Nature Nanotechnology* **2015**, *10*, 459-464, doi:10.1038/nnano.2015.37.
61. Sakong, S.; Kratzer, P. Hydrogen vibrational modes on graphene and relaxation of the C-H stretch excitation from first-principles calculations. *The Journal of Chemical Physics* **2010**, *133*, 054505, doi:10.1063/1.3474806.
62. Miura, Y.; Kasai, H.; Agerico Diño, W.; Nakanishi, H.; Sugimoto, T. Effective Pathway for Hydrogen Atom Adsorption on Graphene. *Journal of the Physical Society of Japan* **2003**, *72*, 995-997, doi:10.1143/JPSJ.72.995.
63. Yan, Z.; Zhu, L.; Li, Y.C.; Wycisk, R.J.; Pintauro, P.N.; Hickner, M.A.; Mallouk, T.E. The balance of electric field and interfacial catalysis in promoting water dissociation in bipolar membranes. *Energy & Environmental Science* **2018**, *11*, 2235-2245, doi:10.1039/C8EE01192C.
64. Cassone, G. Nuclear Quantum Effects Largely Influence Molecular Dissociation and Proton Transfer in Liquid Water under an Electric Field. *The Journal of Physical Chemistry Letters* **2020**, *11*, 8983-8988, doi:10.1021/acs.jpclett.0c02581.
65. Saitta, A.M.; Saija, F.; Giaquinta, P.V. Ab Initio Molecular Dynamics Study of Dissociation of Water under an Electric Field. *Physical Review Letters* **2012**, *108*, 207801, doi:10.1103/PhysRevLett.108.207801.
66. Muñoz-Santiburcio, D.; Marx, D. Nanoconfinement in Slit Pores Enhances Water Self-Dissociation. *Physical Review Letters* **2017**, *119*, 056002, doi:10.1103/PhysRevLett.119.056002.
67. Sirkin, Y.A.P.; Hassanali, A.; Scherlis, D.A. One-Dimensional Confinement Inhibits Water Dissociation in Carbon Nanotubes. *The Journal of Physical Chemistry Letters* **2018**, *9*, 5029-5033, doi:10.1021/acs.jpclett.8b02183.
68. Bepete, G.; Anglaret, E.; Ortolani, L.; Morandi, V.; Huang, K.; Pénicaud, A.; Drummond, C. Surfactant-free single-layer graphene in water. *Nature Chemistry* **2017**, *9*, 347-352, doi:10.1038/nchem.2669.
69. Park, K.A.; Seo, K.; Lee, Y.H. Adsorption of Atomic Hydrogen on Single-Walled Carbon Nanotubes. *The Journal of Physical Chemistry B* **2005**, *109*, 8967-8972, doi:10.1021/jp0500743.

70. Grosjean, B.; Bocquet, M.-L.; Vuilleumier, R. Versatile electrification of two-dimensional nanomaterials in water. *Nature Communications* **2019**, *10*, 1656, doi:10.1038/s41467-019-09708-7.
71. Casolo, S.; Løvvik, O.M.; Martinazzo, R.; Tantardini, G.F. Understanding adsorption of hydrogen atoms on graphene. *The Journal of Chemical Physics* **2009**, *130*, 054704, doi:10.1063/1.3072333.
72. Zhang, Z.W.; Zheng, W.T.; Jiang, Q. Hydrogen adsorption on Ce/SWCNT systems: a DFT study. *Physical Chemistry Chemical Physics* **2011**, *13*, 9483-9489, doi:10.1039/C0CP02917C.
73. Ivanovskaya, V.V.; Zobelli, A.; Teillet-Billy, D.; Rougeau, N.; Sidis, V.; Briddon, P.R. Hydrogen adsorption on graphene: a first principles study. *The European Physical Journal B* **2010**, *76*, 481-486, doi:10.1140/epjb/e2010-00238-7.
74. Jena, N.K.; Tripathy, M.K.; Samanta, A.K.; Chandrakumar, K.R.S.; Ghosh, S.K. Water molecule encapsulated in carbon nanotube model systems: effect of confinement and curvature. *Theoretical Chemistry Accounts* **2012**, *131*, 1205, doi:10.1007/s00214-012-1205-z.
75. Matis, B.R.; Burgess, J.S.; Bulat, F.A.; Friedman, A.L.; Houston, B.H.; Baldwin, J.W. Surface Doping and Band Gap Tunability in Hydrogenated Graphene. *ACS Nano* **2012**, *6*, 17-22, doi:10.1021/nn2034555.
76. Katin, K.P.; Prudkovskiy, V.S.; Maslov, M.M. Chemisorption of hydrogen atoms and hydroxyl groups on stretched graphene: A coupled QM/QM study. *Physics Letters A* **2017**, *381*, 2686-2690, doi:https://doi.org/10.1016/j.physleta.2017.06.017.
77. Lu, Y.; Feng, Y.P. Adsorptions of hydrogen on graphene and other forms of carbon structures: First principle calculations. *Nanoscale* **2011**, *3*, 2444-2453, doi:10.1039/C1NR10118H.